Research Article

Identification of stress regimes by using 1D geomechanical modeling of clastic and carbonate reservoirs

Iftikhar Ahmed Satti[1,2] · **Chen Xin**[2]

Received: 17 June 2020 / Accepted: 29 October 2020 / Published online: 16 November 2020

Abstract
In this paper, data from one well is used for pore pressure prediction and geomechanical modeling in clastic and carbonate reservoirs. Pore pressure is successfully predicted in the clastic and carbonates reservoirs using trend line method. Geomechanical models showed that the direction of maximum horizontal stress is north–south, perpendicular to the direction of borehole breakout propagation. Change in magnitude of principle stresses confirmed the presence of different stress regimes in the study area. From the results of this study, it is inferred that pore pressure prediction and geomechanical modeling will help to reduce the borehole failure problems and determine safe mud window.

Keywords Pore pressure · Geomechanics · Carbonate reservoir · Wellbore stability · In situ stress

1 Introduction

Pore fluid pressure is the pressure exerted by fluids within the confined pore space. Pore pressure higher than the hydrostatic pressure is called overpressure and has significant importance in geohazard analysis [1]. Overpressure can be generated by different mechanisms such as undercompaction and fluid expansion [2]. Eaton's (1972) ratio method [3] and Bower's method [2] are commonly used for pore pressure prediction.

Many problems, such as borehole breakouts, collapse, losses of borehole and increased drilling time, are associated with inaccurate wellbore stability analysis [4]. The signs of stress concentration around the borehole are distinguished by compressive and tensile-induced failure which can occur at both sides of the borehole wall where stress concentration has exceeded the strength of the rock [5].

Image log is widely used for interpretation of axial tensile-induced and compressive (breakout) failures which are reliable indicators of the minimum and maximum horizontal in situ stress orientation, respectively. The mechanical instabilities in the borehole during the drilling can be reduced or mitigated by choosing the optimal mud weight and optimal well bore trajectory [5–7].

The study area is geologically complex, and not enough published literature is available about the orientation and magnitude of in situ stresses. The focus of this paper is to predict pore pressure and prepare 1D geomechanical models of oil and gas bearing clastic and carbonate reservoirs to understand the change in the nature of the stress regimes with depth for targeting the deep reservoirs and better well planning of the future wells. Hence, the present work can be used as a base for further geomechanical modeling work.

2 Methodology

Wireline log, image log and drilling data from one well is used for this study. Eaton's (1972) method is used for pore pressure prediction. Overburden pressure is

✉ Iftikhar Ahmed Satti, iasatti@gmail.com | [1]Institute of Geology, University of Azad Jammu and Kashmir, Muzaffarabad, Pakistan. [2]Geophysical Research Institute of BGP Inc, CNPC, Zhuozhou, China.

calculated using the density log (RHOB), and gamma ray (GR) log is used to discriminate the lithology. Shale points sonic values are used to develop the normal compaction trend and predict the pore pressure. The Eaton's (1972) method is given in Eq. 1:

$$PP = \sigma T - (\sigma T - Pn) * (\Delta tn/\Delta t)^{EE} \quad (1)$$

where PP = predicted pore pressure, σT = total vertical stress, Pn = normal or hydrostatic pressure,

Δt = sonic transit time from well log, Δtn = normal sonic transit time when pore pressure is hydrostatic and EE = Eaton's exponent (for sonic transit time is 3).

The Eaton's (1972) method is empirical, and its regionally defined exponent (the Eaton's exponent) can be easily varied to calibrate the trend to predict the pore pressure generated by different mechanisms [8]. In the sediments, where overpressure is generated by undercompaction mechanisms, an Eaton's exponent of 3.0 is typically used for pore pressure prediction. Poisson's ratio (ν) is calculated from acoustic velocities. The equation for Poisson's ratio calculation is given as:

$$\nu = (Vp^2 - 2Vs^2)/2(Vp^2 - Vs^2) \quad (2)$$

where Vp and Vs are the P-wave and S-wave velocities, obtained from compressional and shear sonic log.

Unconfined compressive strength (UCS) is a critical parameter required to address the geomechanical problems like controlling wellbore instabilities during drilling and quantitatively constrain the magnitude of maximum horizontal stress using wellbore failure observation [9].

Typically, this parameter is obtained from laboratory core test. Since rock mechanical test data were not available, based on the regional geological knowledge, UCS and coefficient of internal friction were calculated using the mathematical equations. The study area consists of different lithologies (i.e., sandstone, shale and limestone) so different equations are used to calculate UCS for each lithology. Militzer-DT [10], *V*p cubed and Hemlock method are used to calculate UCS for limestone, shale and sandstone, respectively [10, 11]. These equations are given as:

$$(\text{Limestone}) : UCS = (7682/DT)^{1.82} \quad (3)$$

$$(\text{Shale/Claystone}) : UCS = 72.5 * Vp^3 \quad (4)$$

$$(\text{Sandstone}) : UCS = 0.001750 * M - 3043 \quad (5)$$

where DT is the sonic transit time (μs/ft), Vp is p-wave velocity in m/s, and M is the P-wave modulus in psi. P-wave modulus is calculated from density (ρ) and sonic velocity, given as

$$M = \rho Vp^2 \quad (6)$$

Young's modulus (E) is the mechanical property that measures the stiffness of the solid material. There are two types (i.e., static and dynamic) of Young's modulus. Dynamic Young's modulus is calculated using the seismic velocities, whereas static Young's modulus is calculated in the laboratories using core data/rock samples. Static and dynamic Young's moduli of rock are normally different. There exists a relationship between static and dynamic Young's moduli, and it depends upon stress path, the stress history and lithology.[12].

In order to use Young's moduli for geomechanical modeling, dynamic Young's moduli should be replaced with static Young's moduli, which requires special laboratory experiments with loading machines of presses. Dynamic Young's modulus is calculated using the following equation:

$$E = \rho Vs^2(3Vp^2 - 4Vs^2)/(Vp^2 - Vs^2) \quad (7)$$

Lal's *V*p (1999) method [11] is used to calculate the coefficient of internal friction (μ). Lal's Vp method is given in Eq. 8:

$$\mu = \tan(sin^{-1}((Vp - 1000)/(VP + 1000))) \quad (8)$$

where μ is the coefficient of internal friction and Vp is P-wave velocity in m/s.

According to Zoback et al. [13], the best measurements of the minimum principal stress can be obtained from the methods such as leak-off test (LOT) that involves the initiation and propagation of hydraulic fractures at depth. Hence, the minimum horizontal stress (SHmin) is determined from the available leak-off test data (LOP).

Image log and four-arm caliper log plot of the well XX is used to identify the borehole breakouts which are then used for the determination of orientation and magnitude of the maximum horizontal stress (SHmax) (Fig. 1).

Rose diagram is prepared using the borehole breakout azimuth (at depth of 2185 m) derived from the image log of the well XX (Fig. 2a, b). Figure 3 shows the rose diagram of the azimuth of all the borehole breakouts derived from image log of well XX.

The stress polygon method and Mohr–Coulomb failure criteria of Moos and Zoback [14] are used to determine the magnitude of SHmax at different depth points in sandstone and limestone. Wellbore stability analysis is performed to constrain geomechanical model through drilling experience, field observation, and field measurement and test data.

Predicted pore pressure, magnitude of in situ stresses and their orientation and rock mechanical parameters such as unconfined compressive strength (UCS), internal

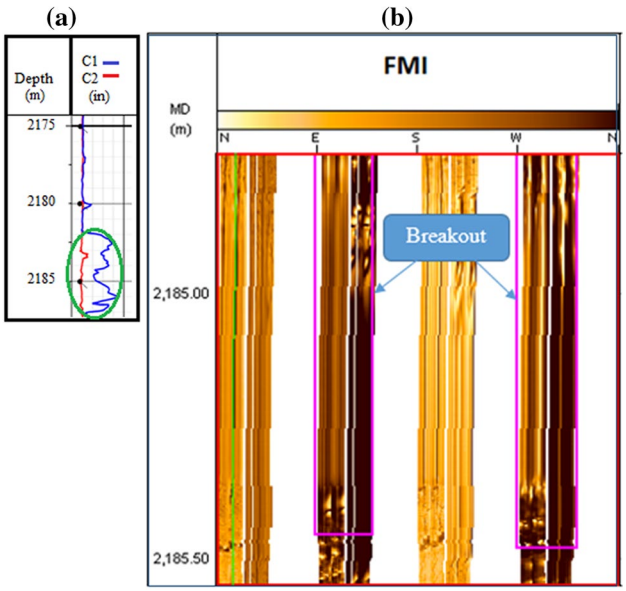

Fig. 1 Example of borehole breakout interpretation using **a** image log and **b** four-arm caliper log plot of the well XX. Separation of caliper one (C1) and caliper two (C2) (green circle) shows the presence of borehole breakout

friction coefficient (IF), Young's modulus (YM) and Poisson's ratio (PR) are used for tendency of breakout initiation and 1D geomechanical modeling.

3 Results and discussions

Pore pressure prediction result of the XX well along with generalized lithology column and gamma ray log is shown in Fig. 4. Pore pressure is successfully predicted in sandstone and limestone using Eaton's (1972) method with an Eaton's exponent of 1.2. Since the repeat formation tester (RFT) data are not available, the predicted pressure is calibrated with mud weight. Since the mud weight is higher than the pore pressure, the calibrated pore pressure is kept slightly lower than the mud weight.

Rose diagram of the interpreted borehole breakout azimuth showed that the azimuth of the identified borehole breakout is 115° ESE and azimuth of the SHmax is N25.29°E. However, borehole breakout propagates in a direction parallel to the SHmin and perpendicular to SHmax. Hence, it is inferred that the orientation of SHmin is ESE-WNW and orientation of SHmax is NNE-SSW.

Stress polygons define possible magnitudes of SHmin and SHmax at any given depth as defined by Anderson's faulting theory and Coulomb faulting theory for a given coefficient of friction and pore pressure. The stress polygon method [13] showed the presence of normal and strike slip fault regimes in clastic (Formation B, depth = 2185 m) and carbonate (Formation D, depth = 3164 m) rocks, respectively (Figs. 5, 6).

Figure 7(a, b) shows the compressive rock strength needed to prevent breakout occurrence at depth of 2185–3164 m, respectively, for any arbitrary well before

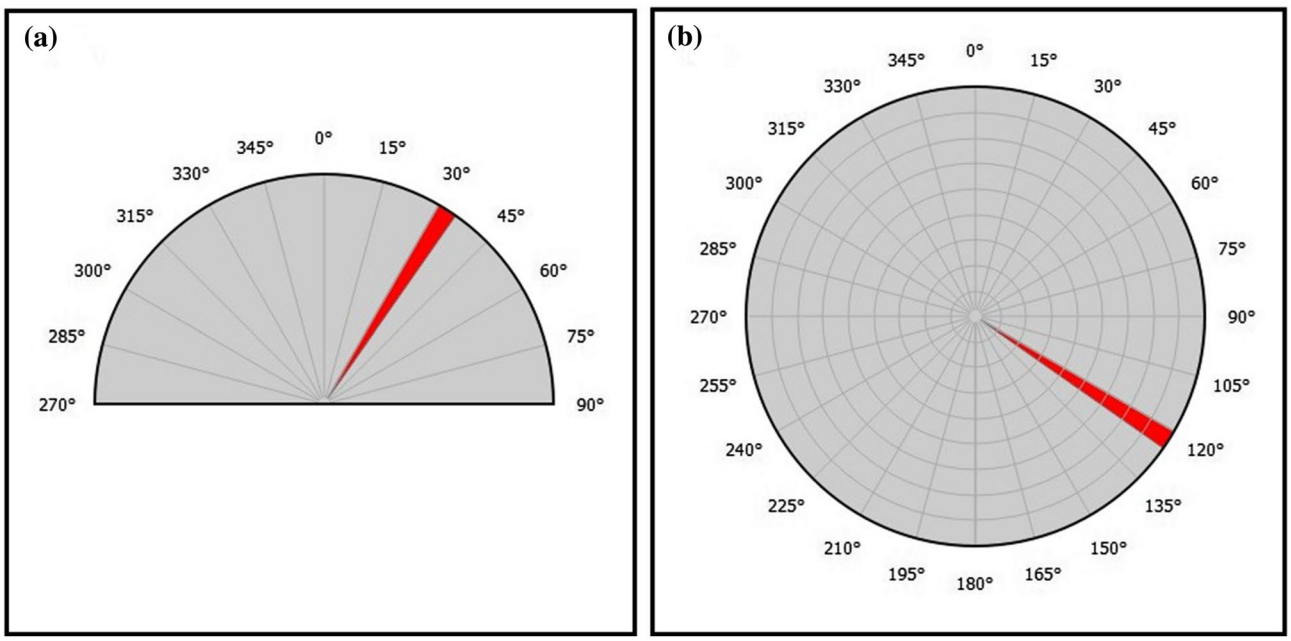

Fig. 2 Rose diagram showing **a** azimuth of the SHmax; **b** azimuth of the identified borehole breakout

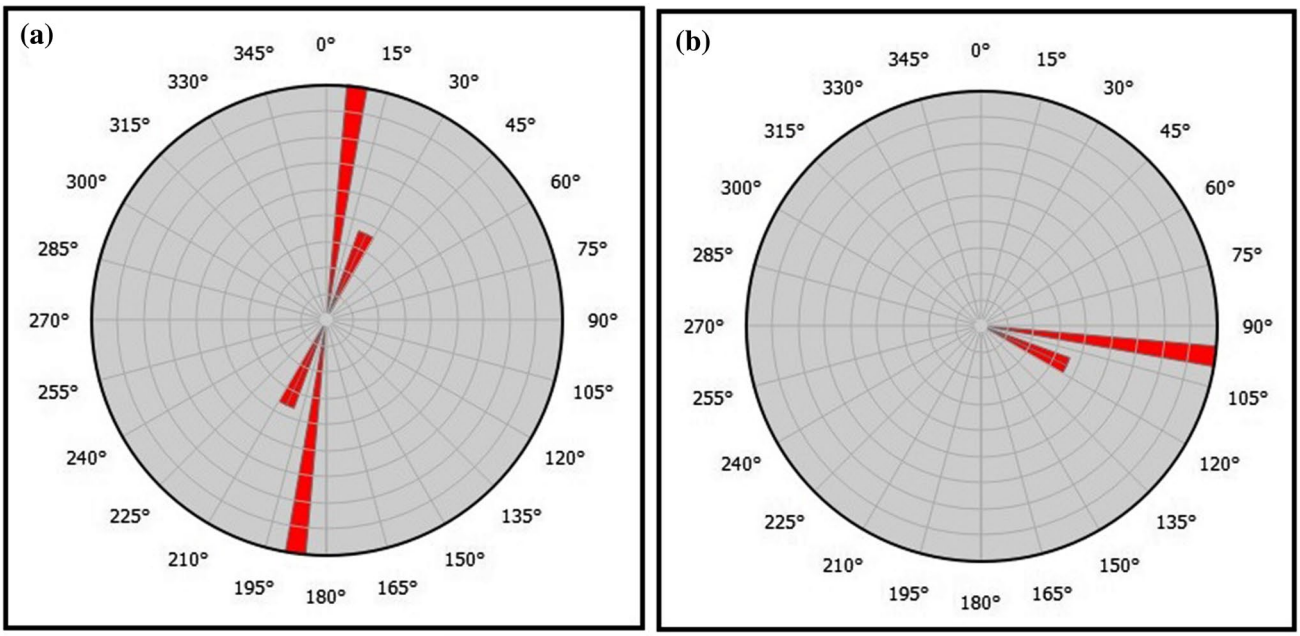

Fig. 3 Rose diagram of all the interpreted borehole breakouts showing **a** azimuth of the SHmax; **b** azimuth of the borehole breakouts

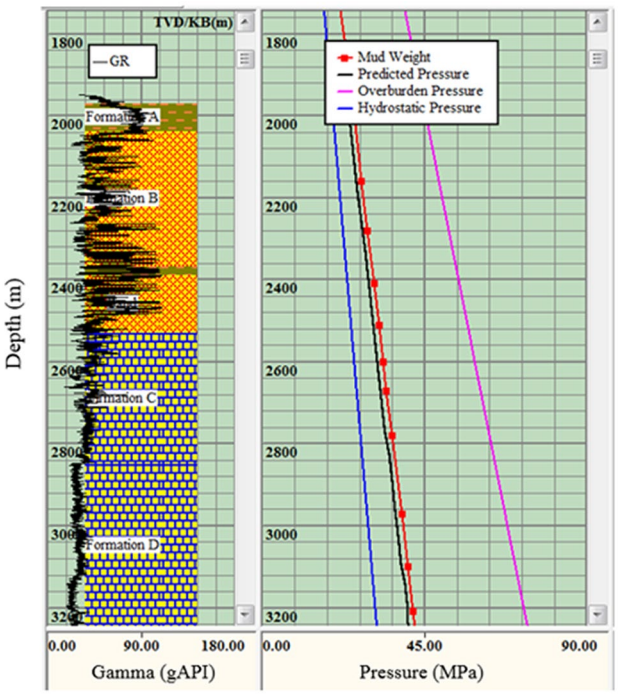

Fig. 4 Pore pressure prediction result of the well XX, compared with mud weight. Black color line is predicted pressure using Eaton's exponent of 1.2. Blue, pink and red color lines are showing hydrostatic pressure, overburden pressure and mud weight, respectively. The hydrostatic pressure gradient is taken as 0.433psi/ft

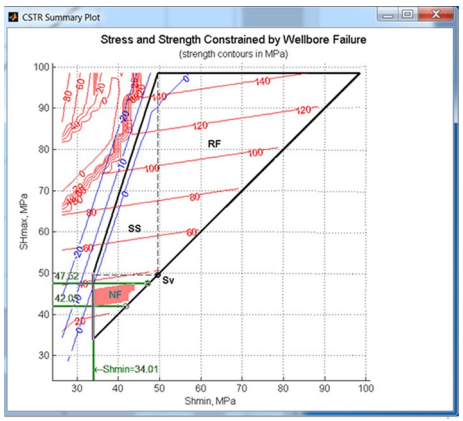

Fig. 5 Example of SHmax magnitude determination using the stress polygon method in clastic rock (sandstone) showed that the magnitude of SHmax is 42.05–47.52 constrained by using the breakout width and UCS. The stress polygon shows that it is the normal faulting regime. The each red color line represents the rock strength given to occur for the breakout with 47.39° width. Blue lines show the possible stress magnitude required to induce drilling-induced tensile fractures

completion of drilling. Red color means that it takes high strength to inhibit failure, while cold (blue) color indicates low rock strength is needed to prevent failure. Vertical boreholes will lie in the center of each plot (i.e., 0° deviation). Figure 7a (tendency for breakout initiation) shows that in the normal faulting regime, higher rock strength is required to drill the horizontal well and limit the breakouts, whereas in the strike slip fault regime (Fig. 7b), it is

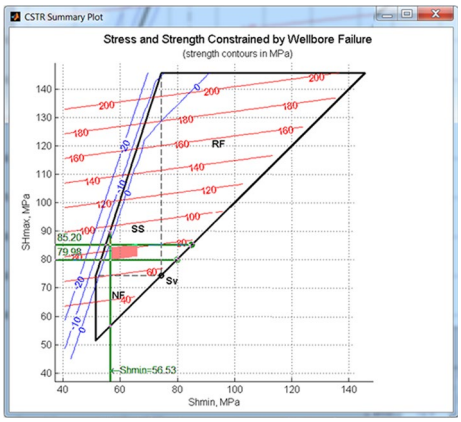

Fig. 6 Example of SHmax magnitude determination using the stress polygon method in carbonate rock (limestone) showed that the magnitude of SH max is 79.98–85.20 constrained by using the braekout width and UCS. The stress polygon shows that it is the strike slip faulting regime. The each red color line represents the rock strength given to occur for the breakout with 49° width. Blue lines show the possible stress magnitude required to induce drilling-induced tensile fractures

reverse case and higher rock strength is required to drill the vertical well.

Breakouts form in the area around a wellbore where the stress concentration exceeds the strength of the rock. Figure 8(a, b) demonstrates the effect of mud weight (Pm) and rock strength (C0) on various modes of borehole failure and conditions for which various modes of compressive failure occur as a function of Pm and C0. These plots are obtained by using the known values of Pm, C0 and breakout width at the given depth points for both (clastic and carbonate) rocks. These plots showed that by increasing the mud weight, the breakout width can be reduced to desired level. But, mud weight should be lower than the minimum horizontal stress (SHmin) to avoid wellbore failure.

Figure 9 shows 1D geomechanical model using available drilling (i.e., mud weight), well test (i.e., LOP) and calculated (i.e., pore pressure, overburden pressure and SHmax) data.

The magnitude of SHmax is increasing quickly with depth, and it is higher than overburden pressure below depth of 2300 m. It is noted that at the depth of ~ 2300 m, normal faulting regime is changing to strike slip faulting regime as SHmax is getting higher than the overburden pressure. The safe mud window is between pore pressure and leak-off pressure (SHmin).

4 Conclusions

Based on the pore pressure prediction and geomechanical modeling results, it is concluded that the pore pressure in the clastic and carbonate reservoirs can be predicted using Eaton's (1972) method. Orientation of the maximum horizontal stress is NNE-SSW, and the orientation of the minimum horizontal stress is ESE-WNW. The magnitude of SHmax is increasing with depth, and faults are changing their nature from normal fault to strike slip fault. This change in nature of faults indicates the presence of different stress regimes that have effect on the

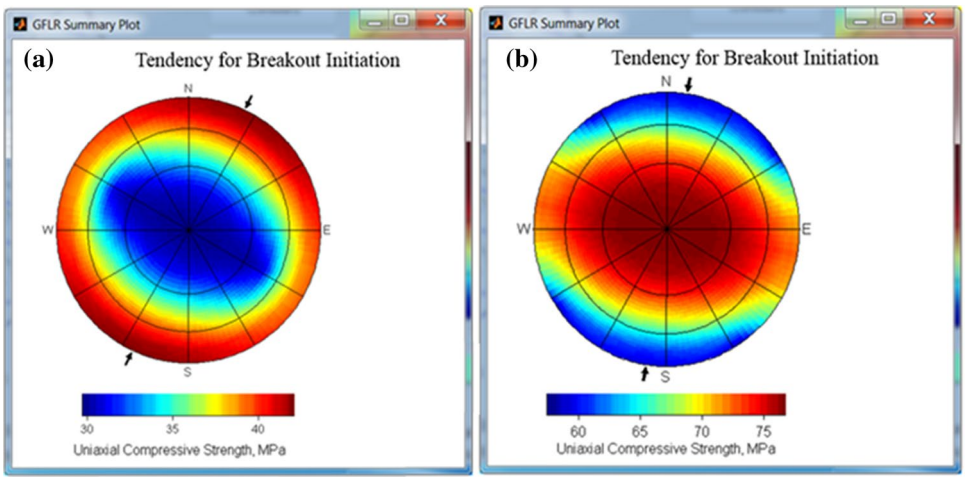

Fig. 7 Example of the tendency for breakout initiation analysis for sandstone (at depth of 2185 m) and limestone (at depth of 3164 m) in normal and strike slip fault regimes, respectively. **a** Rock strength of sandstone required to avoid borehole breakout in normal fault regime is computed to be 30–40 MPa from vertical to horizontal. **b** Rock strength of limestone required to avoid borehole breakout in normal fault regime is computed to be 60–75 MPa from horizontal to vertical. The outer most circle shows the 90° deviation (horizontal) and the black dot in the center of each plot shows 0° deviation (vertical). The black arrows are showing the orientation of the SHmax

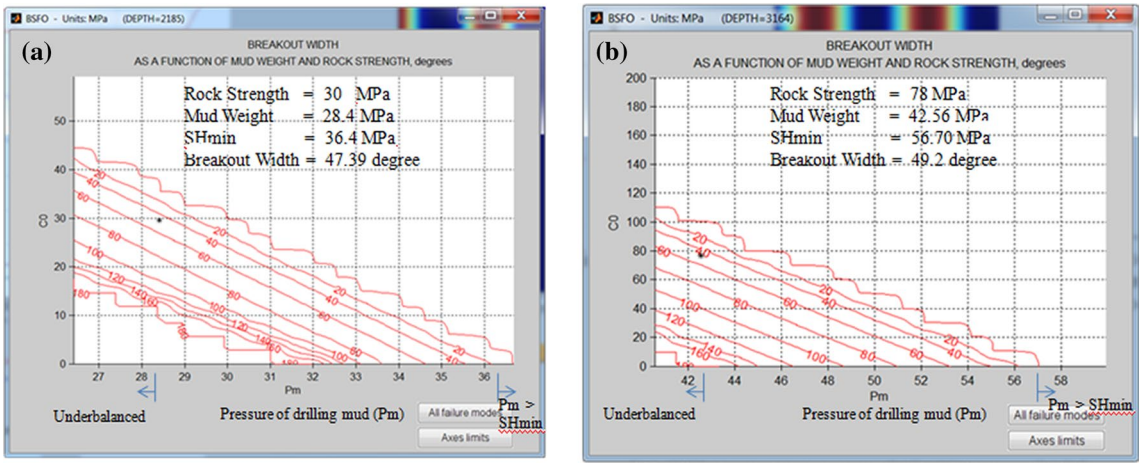

Fig. 8 Example of breakout width (red lines) as a function of mud weight (Pm) on the x-axis and rock strength (C0) on the y-axis: **a** for sandstone **b** for limestone. The small black "* " shows the given value of breakout width (in degrees), mud weight (MPa) and rock strength (MPa) used in this analysis. Red lines show the possible values of breakout width in degrees. For the given rock strength, increase in mud weight will reduce the breakout width

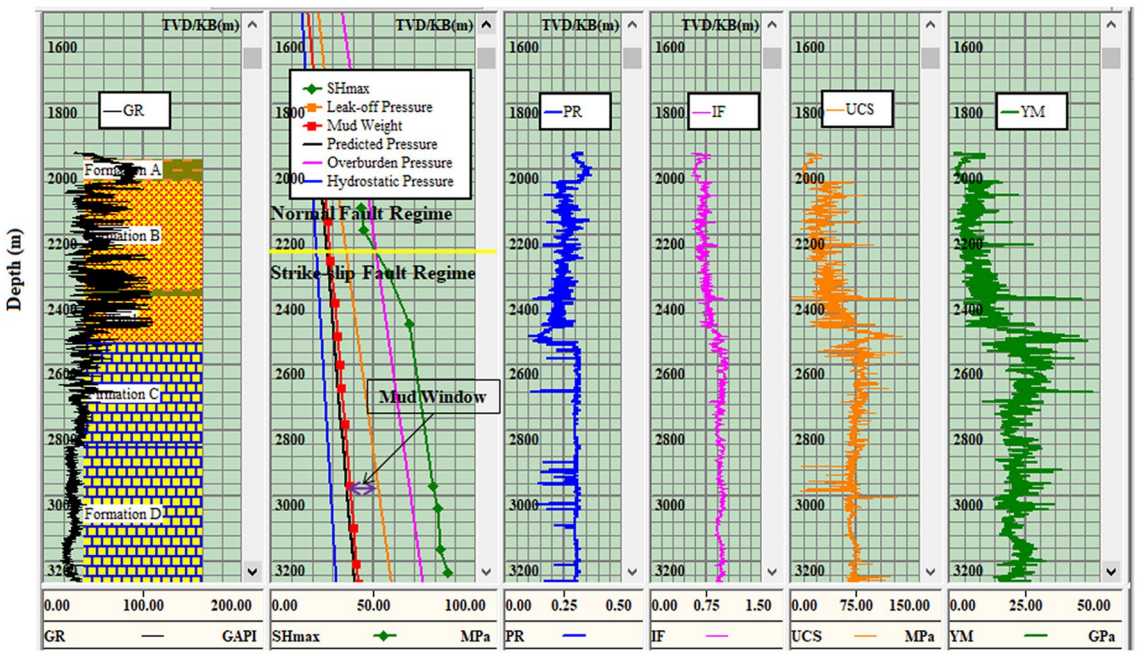

Fig. 9 1D geomechanical model for the well XX showing different stress regimes, hydrostatic pressure (blue line), predicted pore pressure (black line), principal stresses (i.e., leak-off pressure (SHmin), SHmax and overburden pressure), mud weight (red line) and logs of: Poisson's ratio (PR), coefficient of internal friction (IF), unconfined compressive strength (UCS) and Young's modulus (YM)

tendency for breakout initiation during drilling operations. To drill the horizontal well in clastic and vertical well in the carbonate rock, the unconfined rock strength is not enough to limit the breakout propagation. Hence, mud weight can be increased to reduce the width of borehole breakouts and avoid borehole failure. Hence, pore pressure prediction coupled with geomechanical modeling is useful to identify the different stress regimes and determine safe mud window to mitigate mechanical instabilities.

Acknowledgements The authors wish to thank the Geophysical Research Institute for providing the support to carry out this study.

Compliance with ethical standards

Conflict of Interest On behalf of all authors, the corresponding author states that there is no conflict of interest.

References

1. Bowers GL (2002) Detecting high overpressure. Lead Edge 21(2):174–177
2. Bowers GL (1995) Pore pressure estimation from velocity data: Accounting for pore pressure mechanisms besides undercompaction. SPE Drill Completion 10(2):89–95
3. Eatons BA (1972) The Effect of Overburden Stress on Geopressure Prediction from Well Logs. J Petroleum Technol 24(8):929–934
4. Zhang J (2013) Borehole stability analysis accounting for anisotropies in drilling to weak bedding planes. Int J Rock Mech Min Sci 60:160–170
5. Yaghoubi AA, Zeinali M (2009) Determination of magnitude and orientation of the in-situ stress from borehole breakout and effect of pore pressure on borehole stability—Case study in CheshmehKhush oil field of Iran. J Petrol Sci Eng 67:116–126
6. Tingay, M., Reinecker, J., and Müller, B. (2008) Borehole breakout and drilling-induced fracture analysis from image logs. World Stress Map Project, 1–8.
7. Dasgupta T, Dasgupta S, Mukherjee S (2019) Image Log Interpretation and Geomechanical Issues. Teaching Methodologies in Structural Geology and Tectonics. Springer, Singapore, pp 237–251
8. Satti IA, Ghosh DP, W.I.W, Hoesni MJ (2015) Origin of Overpressure in a Field in the Southwestern Malay Basin. SPE Drilling & Completion 30 (3), 198–211.https://library.seg.org/action/doSearch?displaySummary=true&ContribAuthorStored=Ghosh%2C+Deva+PrasadYusoff
9. Hamdi Z, Momeni MS, Meyghani B, Zivar D, Chung BY, Bataee M, Asadian MA (2019) Oil well compressive strength analysis from sonic log; a case study. In IOP Conference Series: Materials Science and Engineering, 495(1), 12077. IOP Publishing .
10. Militzer H, Stoll R (1973) EinigeBeitrageder geophysics zurprimadatenerfassungimBergbau. NeueBergbautechnik Leipzig 3(1):21–25
11. Lal M (1999) Shale stability: drilling fluid interaction and shale strength, SPE 54356. SPE Latin American and Carribean Petroleum Engineering Conference, Caracas, Venezuela, Society of Petroleum Engineering.
12. Fjær E (2019) Relations between static and dynamic moduli of sedimentary rocks. Geophys Prospect 67(1):128–139
13. Zoback MD, Barton CA, Brudy M, Castillo DA, Finkbeiner T, Grollimund BR, Moos DB, Peska P, Ward CD, Wiprut DJ (2003) Determination of stress orientation and magnitude in deep wells. Int J Rock Mech Min Sci 40:1049–1076
14. Moos D, Zoback MD (1990) Utilization of observations of well bore failure to constrain the orientation and magnitude of crustal stresses: Application to continental, Deep Sea Drilling Project, and Ocean Drilling Program boreholes. J Geophys Res 95(B6):9305–9325